



Original Article

The essential role of *Mkx* in periodontal ligament on the metabolism of alveolar bone and cementum

Lisa Yagasaki ^{a, b}, Tomoki Chiba ^b, Ryota Kurimoto ^b, Mitsuyo Nakajima ^b,
Takanori Iwata ^{a, **}, Hiroshi Asahara ^{b, c, *}

^a Department of Periodontology, Graduate School of Medical and Dental Sciences, Tokyo Medical and Dental University, 1-5-45 Yushima, Bunkyo-ku, Tokyo 113-8510, Japan

^b Department of Systems BioMedicine, Tokyo Medical and Dental University, 1-5-45 Yushima, Bunkyo-ku, Tokyo 113-8519, Japan

^c Department of Molecular and Experimental Medicine, The Scripps Research Institute, La Jolla, CA 92037, USA

ARTICLE INFO

Article history:

Received 25 September 2023

Received in revised form

24 November 2023

Accepted 17 December 2023

Keywords:

Mohawk homeobox (*Mkx*)

Periodontal ligament (PDL)

Ossification

Cementum

Knockout rat

ABSTRACT

Introduction: The periodontium is a connective tissue which consists of periodontal ligament, alveolar bone, cementum and gingiva. Periodontal ligament (PDL) is a specialized connective tissue that connects the cementum – coating the surface of the tooth – to the alveolar bone. Mohawk homeobox (*Mkx*) is a transcription factor that is expressed in PDL, that is known to play a vital role in the development and homeostasis of PDL. A detailed functional analysis of *Mkx* in the periodontal ligament for alveolar bone and cementum metabolism has not yet been conducted.

Materials and methods: Alveolar bone height, bone mineral density (BMD) and bone volume fractions (Bone volume/Total volume: BV/TV) were measured and analyzed using micro-computed tomography (Micro-CT) and 3DBon on 7-week-old male wild-type (WT) (*Mkx*^{+/+}) (n = 10) and *Mkx*-knockout (*Mkx*^{-/-}) (n = 6) rats. Hematoxylin and Eosin (H&E), tartrate-resistant acid phosphatase (TRAP), alkaline phosphatase (ALP) and Masson Trichrome staining were performed on 5, 6, and 7-week-old *Mkx*^{+/+} and *Mkx*^{-/-} rats. Cementum surface area and the number of TRAP-positive osteoclasts/mm were quantified, measured, and compared for 5, 6 and 7-week-old *Mkx*^{+/+} and *Mkx*^{-/-} rats (n = 3 each).

Results: The level of alveolar bone height was significantly higher in *Mkx*^{-/-} rats than in *Mkx*^{+/+} rats. On the other hand, there was significantly less BMD in *Mkx*^{-/-} alveolar bone. A significant increase in cellular cementum could be observed as early as 5 weeks in *Mkx*^{-/-} rats when compared with *Mkx*^{+/+} rats of the same age. More TRAP-positive osteoclasts were observed in *Mkx*^{-/-} rats.

Conclusion: Our findings further reveal the essential roles of *Mkx* in the homeostasis of the periodontal tissue. *Mkx* was found to contribute to bone and cementum metabolism and may be essential to the prevention of diseases such as periodontitis, and could show potential in regenerative treatments.

© 2023, The Japanese Society for Regenerative Medicine. Production and hosting by Elsevier B.V. This is an open access article under the CC BY-NC-ND license (<http://creativecommons.org/licenses/by-nc-nd/4.0/>).

Abbreviations: PDL, Periodontal ligament; *Mkx*, Mohawk homeobox; BMD, Bone mineral density; BV/TV, Bone volume / Total volume, bone volume fractions; Micro-CT, Micro-computed tomography; WT • *Mkx*^{+/+}, Wild type; *Mkx*^{-/-}, *Mkx*-knockout; H&E, Hematoxylin and Eosin; TRAP, Tartrate-resistant acid phosphatase; ALP, Alkaline phosphatase; MSCs, Mesenchymal stem cells; CEJ, Cemento-enamel junction; ABC, Alveolar bone crest; CO₂, Carbon dioxide; PBS, Phosphate-buffered saline; SEM, Standard errors of the mean; BMC, Bone mineral content; ECM, Extracellular matrix; WHO, World Health Organization; FGFs, Fibroblast growth factors; BMP, Bone morphogenetic protein; SHH, Sonic hedgehog; EDA, Ectodysplasin; PTH, Parathyroid hormone; PTHrP, PTH-related protein; PTH1R, PTH-1 receptor; PTHLH, PTH-like hormone.

* Corresponding author. Department of Systems BioMedicine, Tokyo Medical and Dental University, 1-5-45 Yushima, Bunkyo-ku, Tokyo 113-8510, Japan.

** Corresponding author.

E-mail addresses: iwata.peri@tmd.ac.jp (T. Iwata), asahara.syst@tmd.ac.jp (H. Asahara).

Peer review under responsibility of the Japanese Society for Regenerative Medicine.

<https://doi.org/10.1016/j.reth.2023.12.007>

2352-3204/© 2023, The Japanese Society for Regenerative Medicine. Production and hosting by Elsevier B.V. This is an open access article under the CC BY-NC-ND license (<http://creativecommons.org/licenses/by-nc-nd/4.0/>).

1. Introduction

The periodontium is a connective tissue which consists of periodontal ligament (PDL), alveolar bone, cementum and gingiva. Periodontium provides physical support to teeth and also protects teeth from bacterial damage [1,2]. PDL is primarily composed of type I collagen and connects the cementum to the alveolar bone via Sharpey fibers. PDL protects teeth and alveolar bone from various physical forces, such as those generated from mastication, tongue motions during speech, and orthodontic tooth movement [3]. PDL contains cells such as fibroblasts, osteoblasts, cementoblasts, osteoclasts, endothelial cells and mesenchymal stem cells (MSCs) [3,4].

The cementum is a calcified tissue that covers the surface of the tooth. It does not contain blood vessels or nerves and therefore has low metabolism compared to bone. The primary role of cementum is tooth anchorage to the alveolar bone with the principal fibers. They also aid in tooth eruption and movement by reshaping as well as expanding the root surface. Additionally, cementum compensates crown wear with root expansion [5]. The alveolar bone contains tooth sockets and the supporting alveolar bone structure is composed of cortical and trabecular bone.

Mohawk homeobox (*Mkx*) is a transcription factor expressed in tendons and ligaments that are rich in type 1 collagen and is an essential player for their development and homeostasis. Experiments have shown that *Mkx*-deficient mice and rats exhibited hypoplastic tendons and heterotopic ossification of Achilles' tendons [6,7]. Furthermore, our previous findings showed that *Mkx* is also specifically expressed in PDL and the lack of *Mkx* in mice resulted in degenerative changes in PDL, demonstrating its importance in PDL homeostasis [8]. We also reported that a single-cell RNA-sequencing analysis comparing PDL from *Mkx*-knockout (*Mkx*^{-/-}) and wild-type (*Mkx*^{+/+}) rats revealed the upregulation of ossification-related genes in mesenchymal cell and osteoblast clusters of *Mkx*^{-/-}. Additionally, an increase in both the number and expression of inflammatory mediators in *Mkx*^{-/-} macrophage clusters was observed. These results indicated the possible involvement of *Mkx* in both periodontitis and ankylosis [9]. Based on these findings, we became interested in the precise role of *Mkx* in the periodontal ligament on the neighboring alveolar bone and cementum. In this study, we found that *Mkx*^{-/-} rats had a significantly higher alveolar bone but lower bone mineral density (BMD) compared to *Mkx*^{+/+} rats at its original state. Also, interestingly, a histological analysis of these rats showed a great increase in cellular cementum and increase in the number of TRAP-positive osteoclasts with age in *Mkx*^{-/-} rats, starting as early as 5 weeks. Our results highlight the importance of *Mkx* in PDL in regulating ossification as well as BMD.

2. Materials and methods

2.1. Animals

Mkx^{-/-} rats utilized for this study were generated in a previous study [7] by targeting the nucleotides downstream of the start codon and deleting them in the second exon using the CRISPR/Cas9 system. The control Wistar rats (*Mkx*^{+/+}) were purchased from Sankyo Lab Service (Tokyo, Japan). In this experiment, 7-week-old *Mkx*^{+/+} (n = 10) and *Mkx*^{-/-} (n = 6) rats were used for micro-CT imaging analysis and 5,6,7-week-old *Mkx*^{+/+} and *Mkx*^{-/-} (n = 3 each) rats were used for histological analysis. All animal experiments were performed in accordance with the protocols approved by the Institutional Animal Care and Use Committee of the Tokyo Medical and Dental University (Approval no. A2023-118C2 and G2023-027C).

2.2. Micro-CT imaging analysis

Micro-CT imaging of the maxilla was performed using the microfocus X-ray system (inspeXio SMX-100 CT® SHIMADZU, Tokyo, Japan). The settings used were 75 kV tube voltage and 140 μ A tube current. 3DBon (Ratoc System Engineering Corporation, Tokyo, Japan) was used to obtain a three-dimensional image to determine the alveolar bone height of the right maxillary second molar (M2), BMD and BV/TV.

Alveolar bone height can be measured as the distance from the cemento-enamel junction (CEJ) to the alveolar bone crest (ABC). CEJ-ABC distances were measured linear to the mesial-buccal cusp, buccal groove and distal buccal cusp (Fig. 1a). In the past study, these sites have been confirmed to show susceptibility to bone loss [10]. For each sample, the average of these three measurements were used. Pseudo-colouring of the three-dimensional illustration was performed to clarify the location of the CEJ.

To measure BMD and BV/TV, the same pre-selected 0.4 mm³ region was applied for all samples. All three cross-sections of the

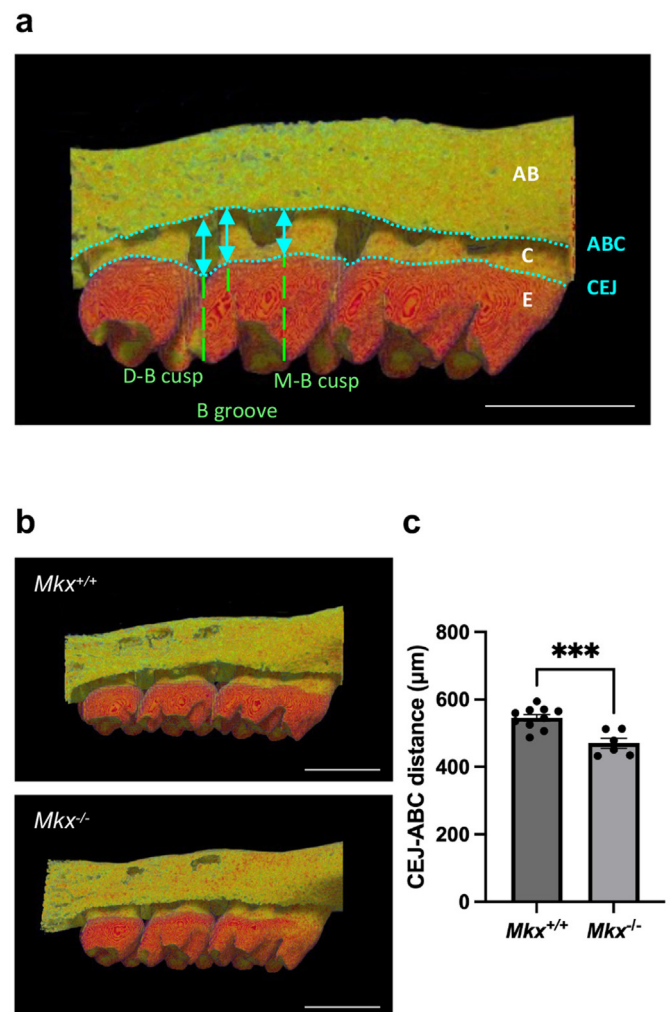


Fig. 1. Alveolar bone height in *Mkx*^{+/+} and *Mkx*^{-/-} rats. (a) Anatomical sites used for deducing the alveolar bone height. Cemento-enamel junction (CEJ) to alveolar bone crest (ABC) distances were measured linear to the mesial-buccal cusp (M-B cusp), buccal groove (B groove) and distal buccal cusp (D-B cusp). Alveolar bone (AB), cementum (C) and enamel (E), (scale bar, 2 mm). (b) Representative portion of the maxilla of *Mkx*^{+/+} and *Mkx*^{-/-} rats, (scale bar, 2 mm). (c) Quantification of the CEJ-ABC distances in each group (*Mkx*^{+/+} n = 10, *Mkx*^{-/-} n = 6). The alveolar bone height was significantly higher in *Mkx*^{+/+}. Data is represented as the mean \pm SEM; ****P* \leq 0.001.

two-dimensional micro-CT view of the maxilla were aligned so that it lay horizontal with X,Y, Z axial lines. The Y-axis was set to cut through the middle of the mesial root of the first molar and the space between the buccal and palatal roots of M2. The X-axis was leveled so that the mesial root of the third molar was in complete view. The Z-axis was positioned in the space between the M2 mesial and distal roots. Finally, the region for selection was positioned central to these axial lines (Fig. 2c).

All measurements were taken twice by two individuals in a blinded manner and the average of both measurements was used for the analysis. The adequacy of the sample size for micro-CT imaging analysis was checked with G*Power, version 3.1.9.6 [11]. The power size obtained was 0.98, which is deemed satisfactory.

2.3. Histological analysis

The rats were euthanized by carbon dioxide (CO₂) inhalation. The sample was fixed in zinc formalin fixative, pH6.25 for 48 h at room temperature. Once the sample was washed with phosphate-buffered saline (PBS), OSTEOSOFT® with 1% zinc sulfate was used to demineralize the sample for approximately 4 weeks. The samples were then paraffin-embedded following standard procedures. Paraffin blocks were sectioned and stained by Genostaff Co., Ltd. All sections were sliced at 4 μm thickness and stained with Hematoxylin and Eosin (H&E) (Hematoxylin: Sigma-Aldrich H9627, Eosin Y:

Sigma-Aldrich E6003, sodium iodate: Nacalai Tesque 31,521–62, aluminium potassium sulfate: Nacalai Tesque 01727–25, citric acid: Nacalai Tesque 09109–85, chloral hydrate: Sigma-Aldrich 05-2660-5), Masson Trichrome (Hematoxylin: Sigma-Aldrich H9627, Weigert's Iron Hematoxylin Liquid 2: Muto Pure Chemicals 4035, mordant: Muto Pure Chemicals 4006, Masson's dye solution A: Muto Pure Chemicals 4016, 0.75% orange G solution: Muto Pure Chemicals 4023, Aniline blue: Muto Pure Chemicals 4020, 12Molybdo (VI) phosphoric Acid n-Hydrate: Nacalai Tesque 27,615, 12Tungsto (VI) Phosphoric Acid n-Hydrate: Nacalai Tesque 27,807, hydrochloric acid: Nacalai Tesque 18,321, acetic acid: Nacalai Tesque 00212), tartrate-resistant acid phosphatase (TRAP) and alkaline phosphatase (ALP) (TRAP/ALP stain kit: Fujifilm Wako Pure Chemical Corporation 296–67001, 2-Amino-2-methyl-1,3-propanediol: Fujifilm Wako Pure Chemical Corporation 015–06411).

Cellular cementum surface area was measured on H&E stained sample images using ImageJ software, version 1.53. For each sample, cellular cementum found on the surface of M2 mesial and distal roots were measured twice each by two individuals in a blinded manner and the average value was recorded. Finally, the averages were combined to produce a value for the total cellular cementum surface area of a sample. This was performed on three different *Mkx*^{+/+} and *Mkx*^{-/-} rats for each of the time points, and the average and the standard errors of the mean (SEM) of the total cellular cementum surface area was calculated and used for the analysis.

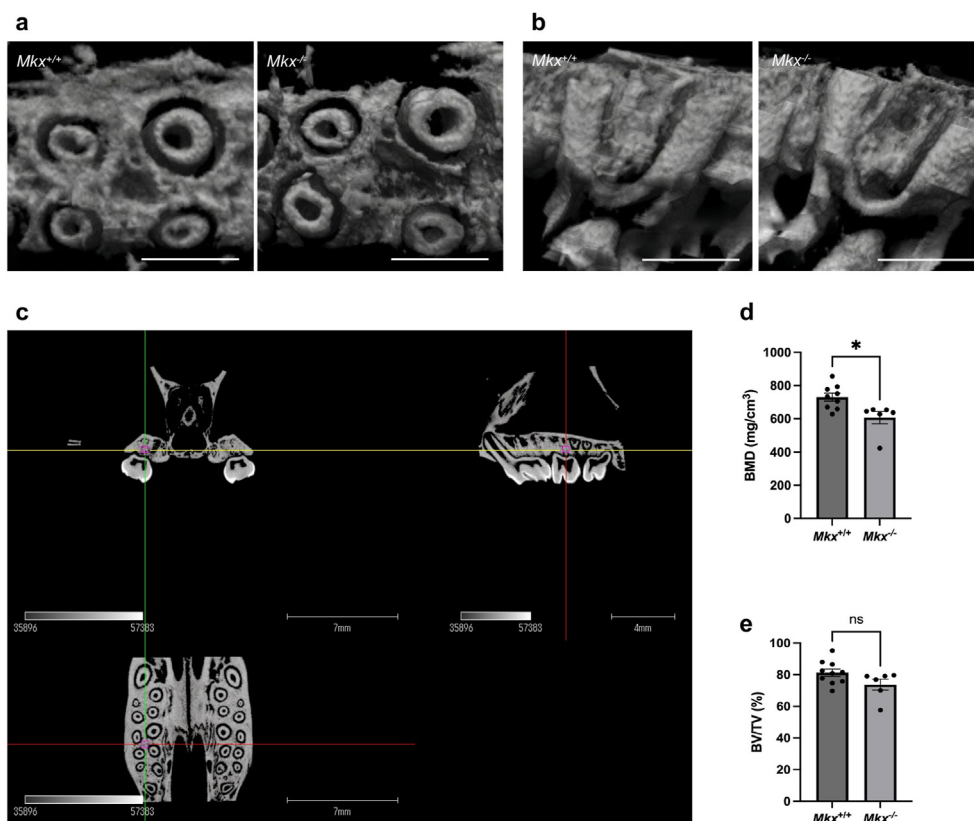


Fig. 2. The effects of *Mkx* on bone mineral density (BMD) and bone volume fraction (BV/TV). (a) A horizontal section through the right maxilla M2, (scale bar, 1 mm). Pronounced bone scarcity observed in between the four roots in *Mkx*^{-/-}. (b) A sagittal section through the right maxilla M2, (scale bar, 1 mm). Pronounced bone scarcity observed in between the two buccal roots in *Mkx*^{-/-}. (c) Cross-sections (X,Y,Z axial lines) of the two-dimensional micro-CT view of the maxilla. Y-axis (green) cuts through the middle of the mesial root of the first molar and the space between roots of M2. X-axis (yellow) was leveled so that the distal root of the third molar was in complete view. The Z-axis (red) was positioned in the space between M2 mesial and distal roots. Finally, the region for selection was positioned central to these axial lines (pink box). (d) Comparison of BMD (mg/cm³) between *Mkx*^{+/+} (n = 10) and *Mkx*^{-/-} (n = 6) in a pre-set region of 0.4 mm³ in between the roots of the maxillary M2. BMD was significantly higher in *Mkx*^{+/+}. (e) Comparison of BV/TV (%) using the same samples and selected regions used for measuring BMD. No significant difference was observed amongst the two types of rats, but a higher BV/TV trend could be seen in *Mkx*^{+/+}. Data is represented as the mean ± SEM; **P* ≤ 0.05, ns: not significant.

The number of TRAP-positive osteoclasts observed on the alveolar bone surface surrounding the M2 root were divided by the total alveolar bone surface length in order to calculate the number of osteoclasts/mm. Total alveolar bone surface length was calculated as the combined length of bone a) on the mesial side of the M2 mesial root, b) on the distal side of the M2 distal root, c) in between the roots of M2, and d) on the alveolar bone surface at the base of M2 tooth. Measurements were taken in a blinded manner in the same process as described above. This process was performed on three individual samples each for $Mkx^{+/+}$ and $Mkx^{-/-}$ rats for 5, 6 and 7 weeks of age.

2.4. Statistical analysis

All results are expressed as the mean \pm SEM. An unpaired two-tailed student's *t*-test was performed to compare two independent groups. Statistical significance was set at $*P \leq 0.05$, $**P \leq 0.01$, and $***P \leq 0.001$. GraphPad Prism, version 9 for Mac (GraphPad Software, San Diego, California, USA) was used to analyze data.

3. Results

3.1. Increased alveolar bone height in $Mkx^{-/-}$ rats

In order to determine the effects of *Mkx* on alveolar bone levels, the CEJ-ABC distance was compared between $Mkx^{+/+}$ and $Mkx^{-/-}$ rats (Fig. 1b). Alveolar bone height can be measured through CEJ-ABC distance, as a smaller CEJ-ABC distance corresponds directly to a higher outer alveolar bone wall. The CEJ-ABC distance average was 550 μm in $Mkx^{+/+}$ rats and 460 μm in $Mkx^{-/-}$ rats. The student *t*-test confirmed a significant increase in alveolar bone height in $Mkx^{-/-}$ rats ($P = 0.0008$) (Fig. 1c). The rat with the highest average alveolar bone height observed was a CEJ-ABC distance of 480 μm in $Mkx^{+/+}$, whereas the distance was 410 μm in $Mkx^{-/-}$. The lowest average alveolar bone height observed on the other hand was a CEJ-ABC distance of 600 μm in $Mkx^{+/+}$, and 530 μm in $Mkx^{-/-}$ rats. This means that the outer wall of the alveolar bone for $Mkx^{-/-}$ rats is higher and therefore appears to cover more tooth surface.

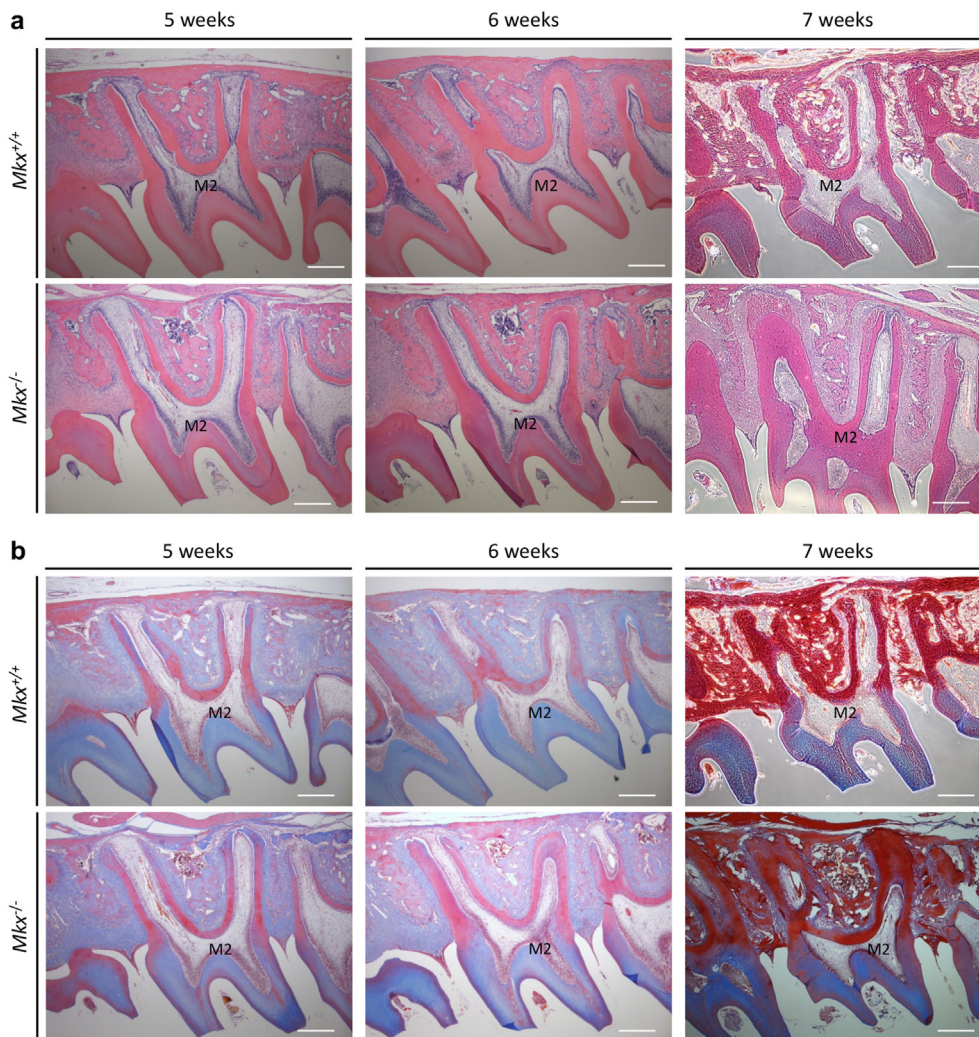


Fig. 3. Histological analysis of the periodontium. (a) H&E staining of $Mkx^{+/+}$ and $Mkx^{-/-}$ rat periodontium at ages 5, 6 and 7 weeks. (b) Masson Trichrome staining of $Mkx^{+/+}$ and $Mkx^{-/-}$ rat periodontium at ages 5, 6 and 7 weeks. Second molar (M2), (Scale bar, 400 μm).

3.2. Lack of *Mkx* results in lower bone mineral density

To further investigate the increase in alveolar bone height in *Mkx*^{-/-} rats, we decided to investigate bone mineral density (BMD). BMD measurements, calculated as Bone mineral content (BMC)/Bone volume (BV), were used to compare the trabecular mineral density in *Mkx*^{+/+} and *Mkx*^{-/-} rat alveolar bone. A pre-set region of 0.4 mm³ in size, in between the roots of the maxillary M2 was measured for BMD (Fig. 2a, b, c). We found that the trabecular bone of *Mkx*^{+/+} rats had significantly more BMD than *Mkx*^{-/-} rats (*P* = 0.0117) (Fig. 2d). A similar pattern was observed for BV/TV (Bone volume/Tissue volume), which shows bone density (Fig. 2e). The findings suggest the involvement of *Mkx* in managing the mineral density and quality of the alveolar bone as well as its ossification.

3.3. Histological analysis shows no distinguished difference in PDL between *Mkx*^{+/+} and *Mkx*^{-/-} rats

To analyze the detailed morphological changes of the periodontium, H&E and Masson Trichrome staining was conducted (Fig. 3). Masson Trichrome stains PDL collagen fibers blue, while bone is stained red. As shown in Fig. 3, the absence of *Mkx* does not appear to show any significant change in PDL within the selected age slots (5 weeks–7 weeks after birth), although changes may appear at a later stage.

3.4. Increase in cellular cementum in *Mkx*^{-/-} rats

Cementum can be defined as either cellular or acellular cementum depending on the presence of cementocytes within the

cementum. Acellular cementum is mainly found on the cervical 1/2~2/3 of the root, whereas cellular cementum can be found on 1/2~2/3 of the apical portion of the root and in furcation areas, containing cementocytes. Cementocytes are cementoblasts embedded in cementoids, which are an unmineralized extracellular matrix (ECM) secreted by cementoblasts during cellular cementum formation [12,13].

While cementum ordinarily increases in thickness towards the apex, a greater increase in cellular cementum volume in 2/3 of the root apex was observed as early as 5 weeks in *Mkx*^{-/-} rats compared with *Mkx*^{+/+} rats. Although cellular cementum increases with age for both types of rats, the rate of cementum expansion was observed to always be greater for *Mkx*^{-/-} rats at every age analyzed (Fig. 4a). As shown in Fig. 4b, the average cellular cementum surface area at 5 weeks was 60.17 mm² and 105.72 mm² in *Mkx*^{+/+} and *Mkx*^{-/-} rats respectively, whereby a significant increase in cellular cementum was shown (*P* = 0.0033). Significant differences were also observed at 6 weeks (*P* = 0.0074) and 7 weeks (*P* = 0.0373). At 6 weeks, the average cellular cementum surface area was 64.35 mm² and 192.23 mm² in *Mkx*^{+/+} and *Mkx*^{-/-} rats respectively. At 7 weeks the average cellular cementum surface area was 95.42 mm² and 198.98 mm² in *Mkx*^{+/+} and *Mkx*^{-/-} rats respectively.

3.5. More osteoclasts and osteoblasts observed without *Mkx*

TRAP and ALP staining was performed to locate osteoclasts and osteoblasts on the alveolar bone surfaces. Significantly more TRAP-positive multinucleated osteoclasts per mm were observed in *Mkx*^{-/-} rats over *Mkx*^{+/+} rats at all ages analyzed (Fig. 5a–e). As

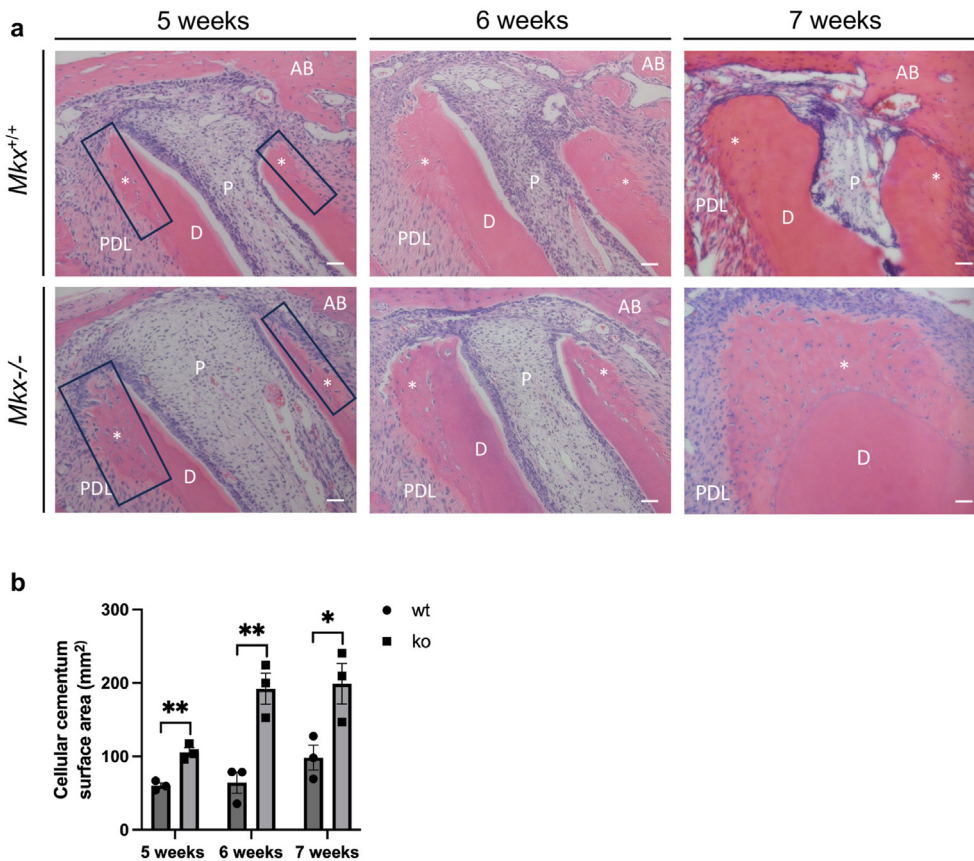


Fig. 4. Difference in the expansion level of cellular cementum at the root apex for *Mkx*^{+/+} and *Mkx*^{-/-} rats with age. (a) H&E staining displaying a greater cellular cementum area in *Mkx*^{-/-} compared with *Mkx*^{+/+} at every age. Cellular cementum (*), Pulp (P), Dentin (D), Periodontal ligament (PDL), Alveolar bone (AB), (Scale bar, 50 μm). (b) A significant increase in cellular cementum surface area (mm²) was observed in *Mkx*^{-/-} in comparison to *Mkx*^{+/+} at 5, 6 and 7-week-old rats. Data represented as the mean ± SEM; **P* ≤ 0.05, ***P* ≤ 0.01.

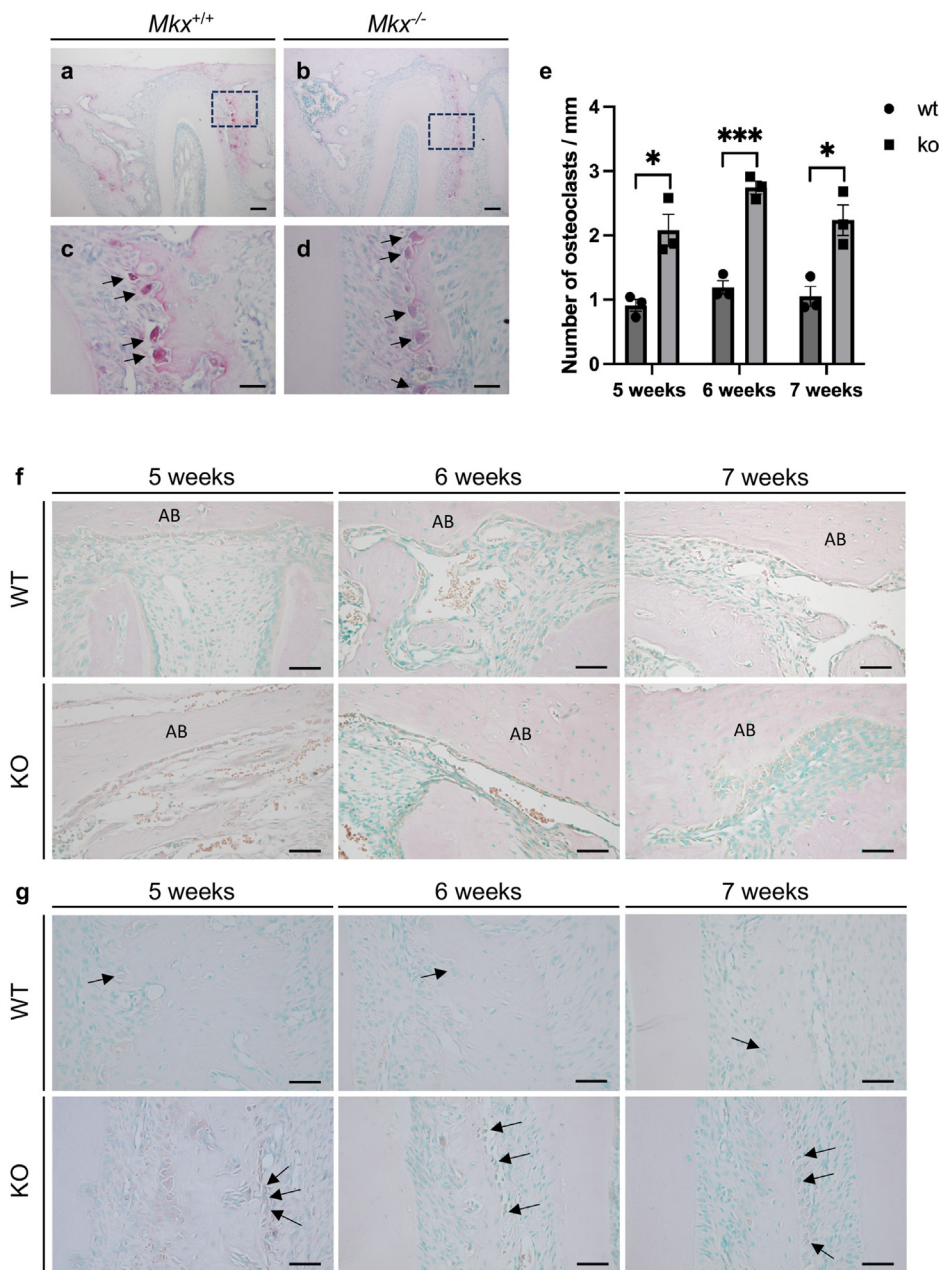


Fig. 5. TRAP and ALP staining of rat periodontium. (a,b) More TRAP-positive multinucleated osteoclasts found on the M2 mesial surface of the distal alveolar bone of a 6-week-old *Mkx*^{-/-} rat (TRAP/ALP; 10x). (c,d) Individual multinucleated TRAP-positive cells indicated with arrows at a higher magnification (TRAP/ALP; 40x) (Scale bar; a,b: 100 μm, c,d: 40 μm). (e) A significant increase in the number of osteoclasts/mm was observed in *Mkx*^{-/-} compared to *Mkx*^{+/+} at 5,6 and 7-week-old rats. Data represented as the mean ± SEM; **P* ≤ 0.05, ****P* ≤ 0.001. (f) Osteoblasts identified on the alveolar bone surface at the base of the M2 tooth for *Mkx*^{+/+} and *Mkx*^{-/-} rats at 5,6 and 7 weeks. Alveolar bone (AB), (ALP; 40x) (Scale bar; 50 μm). (g) More ALP-positive osteoblasts observed in 5,6 and 7-week-old *Mkx*^{-/-} rats. Arrows point at osteoblasts stained brown (ALP; 40x) (Scale bar; 50 μm).

a general trend, there were more osteoclasts on the M2 mesial surface of the distal alveolar bone in comparison to the other alveolar bone surfaces (Fig. 5a–d). The average number of osteoclasts/mm in 5-week-old rats was 0.91 in *Mkx*^{+/+} and 2.08 in *Mkx*^{-/-} (*P* = 0.0122). In 6-week-old rats and 7-week-old rats, they were 1.19 in *Mkx*^{+/+} and 2.74 in *Mkx*^{-/-} (*P* = 0.0005) and 1.05 in *Mkx*^{+/+} and 2.24 in *Mkx*^{-/-} (*P* = 0.0143) respectively (Fig. 5e).

Osteoblasts were identified on the alveolar bone surface at the base of the M2 tooth for both types of rats by ALP staining (Fig. 5f). However, ALP-positive osteoblasts appeared more prominently around the M2 distal alveolar bone surface of 5,6 and 7-week-old *Mkx*^{-/-} rats, while none or very few if any, were detected for *Mkx*^{+/+} rats (Fig. 5g).

4. Discussion

PDL not only attaches teeth to the alveolar bone but it also contains many cells that are vital to the maintenance of the periodontium. Through the utilization of *Mkx*-knockout rats, we have found further evidence to suggest that *Mkx* that is expressed in PDL may be essential in supporting the functional integrity of the periodontium. Interestingly, our findings revealed that *Mkx*^{-/-} rats have a significantly higher alveolar bone height and yet a lower BMD compared to *Mkx*^{+/+} rats. Additionally, we observed a significant increase in cellular cementum and osteoclasts, and a possible increase in osteoblasts in *Mkx*^{-/-} rats.

The increase in alveolar bone height in *Mkx*^{-/-} rats could partially be explained by the effects of *Mkx* deficiency causing heterotopic ossification of the periodontal ligament, as similarly reported by Suzuki et al. [7], Koda et al. [8], Takada et al. [9], and Miyazaki et al. [14]. On the contrary, BMD is significantly reduced and BV/TV also showed a declining pattern for *Mkx*^{-/-} rats in comparison to *Mkx*^{+/+} rats. In this study, BMD shows the quantity of bone mineral in the trabecular portion of the alveolar bone, and can therefore be used to estimate the stiffness and strength of the bone [15]. Such is the case that BMD measurements have been proposed for diagnosing osteoporosis by the World Health Organization (WHO) [16]. Bone density obtained with BV/TV was generally lower in *Mkx*^{-/-} rats, but not to a significant degree. This may be because there is a significant variation in bone density in alveolar bone, as shown in a study using human cadavers [17], making it difficult to obtain results as consistent as those for BMD.

Previously our single-cell RNA-sequencing data revealed a decrease in the expression of *Tnn*, which is important for the extracellular matrix formation in PDL in *Mkx*^{-/-} rats [9]. Also, the study further supported the anti-inflammatory properties of *Mkx*. Lack of *Mkx* causes degradation of the ECM and an increase in inflammatory responses of macrophages [9]. The alteration of ECM leads to an unstable attachment of the tooth to the surrounding structures and therefore a weaker tolerance towards mechanical loading such as those from occlusal and orthodontic forces. Consequently, it can be speculated that the alveolar bone closer to the tooth root experiences more effects from occlusal forces, resulting in the activation of osteoclasts [18]. There were more TRAP-positive cells in *Mkx*^{-/-} rats; in many cases on the distal side of the molars at all of the timepoints covered in this research. This suggests that there were more osteoclasts present in *Mkx*^{-/-} rats than in *Mkx*^{+/+} rats on the distal side, perhaps as a result of the weaker tolerance towards the natural distal drift of the molars [19]. Furthermore, our results appear to support previously published findings that suggest that a lack of *Mkx* leads to an increase in the number of osteoblasts and therefore a promotion in ossification [8,9].

The reduction in BMD and BV/TV in *Mkx*^{-/-} rats observed here correlates with bone rarefaction. Alternatively, an increase in osteoclast numbers in *Mkx*^{-/-} rats could have also been a response to calcium and phosphorus deficiency [20]. The decline in anti-inflammatory responses may also have triggered the increase in osteoclasts and fall in BMD and BV/TV.

Cellular cementum is known to increase its thickness with age and does not usually undergo remodelling, except in responses to mechanical loading from mastication forces, tooth eruption and drifting, orthodontic force and parafunctional gnathic activities [21]. In retrospect, the mechanical force applied on the weakened ECM may have contributed to the cellular cementum expansion in *Mkx*^{-/-} rats. Nevertheless, the phenomenon of increased cellular cementum after knocking out *Mkx* has never been reported and the effect of *Mkx* on cementum is worthy of additional investigation in future studies.

Extracellular matrix composition is similar in bone and teeth, so they share many of the same genes and hormones for their development. For example, signaling pathways involving WNT, fibroblast growth factors (FGFs), bone morphogenetic protein (BMP), sonic hedgehog (SHH) and ectodysplasin (EDA) are required for both tooth and endochondral bone development, and share transcription factors such as Pax9 and Runx2 [21–25]. Parathyroid hormone (PTH), PTH-related protein (PTHrP) and PTH-1 receptor (PTH1R) are known for their importance in root formation and eruption [26,27]. PTH-like hormone (PTHLH) is a PTH receptor ligand, which interestingly was upregulated in *Mkx*^{-/-} rats in our earlier single-cell RNA-sequencing data. It is possible that the

overexpression of PTHLH is one of the contributing factors to a shift in trend towards ossification when *Mkx* is deficient.

Our previous studies have shown that *Mkx* is important in the development and homeostasis of PDL [8,9]. Although abnormal PDL phenotypes *per se* were not observed in this study, the possibility that such phenotypes will appear at later stages remains, as collagen fibril degeneration and an increase in osteogenic gene expression were previously detected in *Mkx*-deficient mice aged 6-months and 12-months respectively. Even though abnormal phenotypes were not observed, another possibility is that scleraxis (*Scx*), another important transcriptional regulator of PDL has helped maintain PDL, since *Scx* has been shown to compensate for the lack of *Mkx* in our former work [8]. However, in our recent study, *Scx* and *Mkx* expression was mutually exclusive, meaning that their roles are different in PDL maintenance [9].

The macro effects of *Mkx* on the periodontium as a whole has been unclear thus far. Through this study, it was possible to further analyze the contribution of *Mkx* on the maintenance of alveolar bone, BMD, trabecular bone density and cementum. Our findings have demonstrated the complex role *Mkx* has on the periodontium, and how its presence in PDL may be essential to the prevention of disease such as periodontitis.

Author contributions

LY planned and performed the study, analyzed data and wrote the manuscript. TC helped design and conceptualize the study, and provide guidance throughout the process. RK provided critical advice. MN helped with the micro-CT imaging and analysis. MI helped with the analysis. TI and HA supervised the study.

Declaration of competing interest

The authors declare that they have no known competing financial interests or personal relationships that could have appeared to influence the work reported in this paper.

Acknowledgements

We thank all members from the Department of Systems BioMedicine and the Department of Periodontology, Tokyo Medical and Dental University for their helpful discussions and support. This work was supported by JSPS KAKENHI (Grant Number JP20H05696), AMED (Grant Numbers JP21gm0810008, JP23gm0010009, JP23ym0126805, JP23ama121045), NIH (Grant Number AR080127 to H.A.) and TMDU Blue-Bird contest (BBC) grant.

References

- [1] Lekic P, McCulloch CA. Periodontal ligament cell population: the central role of fibroblasts in creating a unique tissue. *Anat Rec* 1996;245:327–41.
- [2] Sirisereephap K, Maekawa T, Tamura H, et al. Osteoimmunology in periodontitis: local proteins and compounds to alleviate periodontitis. *Int J Mol Sci* 2022;23:5540.
- [3] Beertsen W, McCulloch CA, Sodek J. The periodontal ligament: a unique, multifunctional connective tissue. *Periodontol* 2000 1997;13:20–40.
- [4] Hosoya A, Shalehin N, Takebe H, et al. Stem cell properties of Gli1-positive cells in the periodontal ligament. *J Oral Biosci* 2020;62:299–305.
- [5] Yamamoto T, Hasegawa T, Hongo H, Amizuka N. Histology of human cementum: its structure, function, and development. *Jpn Dent Sci Rev* 2016;52:63–74.
- [6] Ito Y, Toriuchi N, Yoshitaka T, et al. The Mohawk homeobox gene is a critical regulator of tendon differentiation. *Proc Natl Acad Sci USA* 2010;107:10538–42.
- [7] Suzuki H, Ito Y, Shinohara M, et al. Gene targeting of the transcription factor Mohawk in rats causes heterotopic ossification of Achilles tendon via failed tenogenesis. *Proc Natl Acad Sci USA* 2016;113:7840–5.

- [8] Koda N, Sato T, Shinohara M, et al. The transcription factor mohawk homeobox regulates homeostasis of the periodontal ligament. *Development* 2017;144:313–20.
- [9] Takada K, Chiba T, Miyazaki T, et al. Single cell RNA sequencing reveals critical functions of *Mkx* in periodontal ligament homeostasis. *Front Cell Dev Biol* 2022;10:795441.
- [10] Abe T, Hajishengallis G. Optimization of the ligature-induced periodontitis model in mice. *J Immunol Methods* 2013;394:49–54.
- [11] Faul F, Erdfelder E, Buchner A, Lang AG. Statistical power analyses using G*Power 3.1: tests for correlation and regression analyses. *Behav Res Methods* 2009;41:1149–60.
- [12] Bosshardt DD, Selvig KA. Dental cementum: the dynamic tissue covering of the root. *Periodontol* 2000 1997;13:41–75.
- [13] Zhao N, Foster BL, Bonewald LF. The cementocyte-an osteocyte relative? *J Dent Res* 2016;95:734–41.
- [14] Miyazaki T, Kurimoto R, Chiba T, et al. *Mkx* regulates the orthodontic tooth movement via osteoclast induction. *J Bone Miner Metabol* 2021;39:780–6.
- [15] Turner CH. Bone strength: current concepts. *Ann N Y Acad Sci* 2006;1068:429–46.
- [16] Kanis JA. Assessment of osteoporosis at the primary health-care level. Technical Report. 2008. <http://www.shef.ac.uk/FRAX>.
- [17] Kim YJ, Henkin J. Micro-computed tomography assessment of human alveolar bone: bone density and three-dimensional micro-architecture. *Clin Implant Dent Relat Res* 2015;17:307–13.
- [18] Harrel SK. Occlusal forces as a risk factor for periodontal disease. *Periodontol* 2000 2003;32:111–7.
- [19] Mishima N, Sahara N, Shirakawa M, Ozawa H. Effect of streptozotocin-induced diabetes mellitus on alveolar bone deposition in the rat. *Arch Oral Biol* 2002;47:843–9.
- [20] Thompson ER, Baylink DJ, Wergedal JE. Increases in number and size of osteoclasts in response to calcium or phosphorus deficiency in the rat. *Endocrinology* 1975;97:283–9.
- [21] Kovacs CS, Chaussain C, Osdoby P, Brandi ML, Clarke B, Thakker RV. The role of biomineralization in disorders of skeletal development and tooth formation. *Nat Rev Endocrinol* 2021;17:336–49.
- [22] Thesleff I. Epithelial-mesenchymal signalling regulating tooth morphogenesis. *J Cell Sci* 2003;116:1647–8.
- [23] Nishimura R, Hata K, Ikeda F, et al. Regulation of transcriptional network system during bone and cartilage development. *J Oral Biosci* 2015;57:165–70.
- [24] Li J, Parada C, Chai Y. Cellular and molecular mechanisms of tooth root development. *Development* 2017;144:374–84.
- [25] Kobayashi Y, Uehara S, Udagawa N. Roles of non-canonical Wnt signaling pathways in bone resorption. *J Oral Biosci* 2018;60:31–5.
- [26] Philbrick WM, Dreyer BE, Nakchbandi IA, Karaplis AC. Parathyroid hormone-related protein is required for tooth eruption. *Proc Natl Acad Sci USA* 1998;95:11846–51.
- [27] Ono W, Sakagami N, Nishimori S, Ono N, Kronenberg HM. Parathyroid hormone receptor signalling in osterix-expressing mesenchymal progenitors is essential for tooth root formation. *Nat Commun* 2016;7:11277.